Received: 10 May 2018 | Accepted: 25 May 2018
DOI: 10.1002/pip.3040

ACCELERATED PUBLICATION

WILEY PROGRESS IN PHOTOVOLTAICS

Solar cell efficiency tables (version 52)

Martin A. Green[1] | Yoshihiro Hishikawa[2] | Ewan D. Dunlop[3] | Dean H. Levi[4] | Jochen Hohl-Ebinger[5] | Anita W.Y. Ho-Baillie[1]

[1] Australian Centre for Advanced Photovoltaics, University of New South Wales, Sydney 2052, Australia

[2] Research Center for Photovoltaics (RCPV), National Institute of Advanced Industrial Science and Technology (AIST), Central 2, Umezono 1-1-1, Tsukuba, Ibaraki 305-8568, Japan

[3] Directorate C—Energy, Transport and Climate, European Commission—Joint Research Centre, Via E. Fermi 2749, IT-21027 Ispra, VA, Italy

[4] National Renewable Energy Laboratory, 15013 Denver West Parkway, Golden, CO 80401, USA

[5] Department of Characterisation and Simulation/CalLab Cells, Fraunhofer-Institute for Solar Energy Systems, Heidenhofstr. 2,, D-79110 Freiburg, Germany

Correspondence
Martin A. Green, School of Photovoltaic and Renewable Energy Engineering, University of New South Wales, Sydney 2052, Australia.
Email: m.green@unsw.edu.au

Funding information
Japanese New Energy and Industrial Technology Development Organization (NEDO); US Department of Energy (Office of Science, Office of Basic Energy Sciences and Energy Efficiency and Renewable Energy, Solar Energy Technology Program), Grant/Award Number: DE-AC36-08-GO28308

Abstract

Consolidated tables showing an extensive listing of the highest independently confirmed efficiencies for solar cells and modules are presented. Guidelines for inclusion of results into these tables are outlined and new entries since January 2018 are reviewed.

KEYWORDS

energy conversion efficiency, photovoltaic efficiency, solar cell efficiency

1 | INTRODUCTION

Since January 1993, "*Progress in Photovoltaics*" has published 6 monthly listings of the highest confirmed efficiencies for a range of photovoltaic cell and module technologies.[1,2] By providing guidelines for inclusion of results into these tables, this not only provides an authoritative summary of the current state of the art but also encourages researchers to seek independent confirmation of results and to report results on a standardized basis. In version 33 of these tables,[2] results were updated to the new internationally accepted reference spectrum (International Electrotechnical Commission IEC 60904-3, Ed. 2, 2008).

The most important criterion for inclusion of results into the tables is that they must have been independently measured by a recognized test centre listed elsewhere.[1] A distinction is made between 3 different eligible definitions of cell area, total area, aperture area, and designated illumination area, as also defined elsewhere[1] (note that, if masking is used, masks must have a simple aperture, such as square, rectangular, or circular). "Active area" efficiencies are not included. There are also certain minimum values of the area sought for the different device types (above 0.05 cm^2 for a concentrator cell, 1 cm^2 for a 1-sun cell, and 800 cm^2 for a module).

Results are reported for cells and modules made from different semiconductors and for subcategories within each semiconductor grouping (eg, crystalline, polycrystalline, and thin film). From version 36 onwards, spectral response information is included (when possible) in the form of a plot of the external quantum efficiency (EQE) versus wavelength, either as absolute values or normalized to the peak measured value. Current-voltage (IV) curves have also been included where possible from version 38 onwards. A graphical summary of progress over the first 25 years during which the tables have been published has been included in version 51.[1]

Highest confirmed "1-sun" cell and module results are reported in Tables 1–4. Any changes in the tables from those previously published[1] are set in bold type. In most cases, a literature reference is provided that describes either the result reported, or a similar result (readers identifying improved references are welcome to submit to the lead author). Table 1 summarizes the best-reported measurements for "1-sun" (nonconcentrator) single-junction cells and submodules.

Table 2 contains what might be described as "notable exceptions" for "1-sun" single-junction cells and submodules in the above category. While not conforming to the requirements to be recognized as a class record, the devices in Table 2 have notable characteristics that will be of interest to sections of the photovoltaic community, with entries based on their significance and timeliness. To encourage discrimination, the table is limited to

TABLE 1 Confirmed single-junction terrestrial cell and submodule efficiencies measured under the global AM1.5 spectrum (1000 W/m^2) at 25°C (IEC 60904-3: 2008, ASTM G-173-03 global)

Classification	Efficiency (%)	Area (cm^2)	Voc (V)	Jsc (mA/cm^2)	Fill Factor (%)	Test Centre (Date)	Description
Silicon							
Si (crystalline cell)	26.7 ± 0.5	79.0 (da)	0.738	42.65[a]	84.9	AIST (March 17)	Kaneka, n-type rear IBC[3]
Si (multicrystalline cell)	22.3 ± 0.4[b]	3.923 (ap)	0.6742	41.08[c]	80.5	FhG-ISE (August 17)	FhG-ISE, n-type[4]
Si (thin transfer submodule)	21.2 ± 0.4	239.7 (ap)	0.687[d]	38.50[d,e]	80.3	NREL (April 14)	Solexel (35 μm thick)[5]
Si (thin film minimodule)	10.5 ± 0.3	94.0 (ap)	0.492[d]	29.7[d,f]	72.1	FhG-ISE (August 07)	CSG solar (<2 μm on glass)[6]
III-V cells							
GaAs (thin film cell)	28.8 ± 0.9	0.9927 (ap)	1.122	29.68[g]	86.5	NREL (May 12)	Alta devices[7]
GaAs (multicrystalline)	18.4 ± 0.5	4.011 (t)	0.994	23.2	79.7	NREL (November 95)	RTI, Ge substrate[8]
InP (crystalline cell)	24.2 ± 0.5[b]	1.008 (ap)	0.939	31.15[a]	82.6	NREL (March 13)	NREL[9]
Thin film chalcogenide							
CIGS (cell)	**22.9 ± 0.5**	**1.041 (da)**	**0.744**	**38.77[h]**	**79.5**	**AIST (November 17)**	**Solar frontier[10,11]**
CdTe (cell)	21.0 ± 0.4	1.0623 (ap)	0.8759	30.25[e]	79.4	Newport (August 14)	First solar, on glass[12]
CZTS (cell)	10.0 ± 0.2	1.113 (da)	0.7083	21.77[a]	65.1	NREL (March 17)	UNSW[13]
Amorphous/microcrystalline							
Si (amorphous cell)	10.2 ± 0.3[i,b]	1.001 (da)	0.896	16.36[e]	69.8	AIST (July 14)	AIST[14]
Si (microcrystalline cell)	11.9 ± 0.3[b]	1.044 (da)	0.550	29.72[a]	75.0	AIST (February 17)	AIST[15]
Perovskite							
Perovskite (cell)	20.9 ± 0.7[j,k]	0.991 (da)	1.125	24.92[c]	74.5	Newport (July 17)	KRICT[16]
Perovskite (minimodule)	**17.25 ± 0.6[j,l]**	**277 (da)**	**1.070[d]**	**20.66[d,h]**	**78.1**	**Newport (May 18)**	**Microquanta, 7 serial cells[17]**
Perovskite (submodule)	**11.7 ± 0.4[j]**	**703 (da)**	**1.073[d]**	**14.36[d,h]**	**75.8**	**AIST (March 18)**	**Toshiba, 44 serial cells[18]**
Dye sensitized							
Dye (cell)	11.9 ± 0.4[k,m]	1.005 (da)	0.744	22.47[n]	71.2	AIST (September 12)	Sharp[19]
Dye (minimodule)	10.7 ±0.4[k,m]	26.55 (da)	0.754[d]	20.19[d,o]	69.9	AIST (February 15)	Sharp, 7 serial cells[19]
Dye (submodule)	8.8 ±0.3[m]	398.8 (da)	0.697[d]	18.42[d,p]	68.7	AIST (September 12)	Sharp, 26 serial cells[20]
Organic							
Organic (cell)	11.2 ± 0.3[q]	0.992 (da)	0.780	19.30[e]	74.2	AIST (October 15)	Toshiba[21]
Organic (minimodule)	9.7 ± 0.3[q]	26.14 (da)	0.806[d]	16.47[d,o]	73.2	AIST (February 15)	Toshiba (8 series cells)[22]

CIGS, $CuIn_{1-y}Ga_ySe_2$; a-Si, amorphous silicon/hydrogen alloy; nc-Si, nanocrystalline or microcrystalline silicon; CZTSS, $Cu_2ZnSnS_{4-y}Se_y$; CZTS, Cu_2ZnSnS_4; ap, aperture area; t, total area; da, designated illumination area; FhG-ISE, Fraunhofer Institut für Solare Energiesysteme; AIST, Japanese National Institute of Advanced Industrial Science and Technology.

[a]Spectral response and current-voltage curve reported in version 50 of these tables.

[b]Not measured at an external laboratory.

[c]Spectral response and current-voltage curve reported in version 51 of these tables.

[d]Reported on a "per cell" basis.

[e]Spectral responses and current-voltage curve reported in version 45 of these tables.

[f]Recalibrated from original measurement.

[g]Spectral response and current-voltage curve reported in version 40 of these tables.

[h]Spectral response and current-voltage curve reported in the present version of these tables.

[i]Stabilized by 1000-h exposure to 1-sun light at 50°C.

[j]Initial performance. Han[23] and Yang and You[24] review the stability of similar devices.

[k]Average of forward and reverse sweeps at 150 mV/second (hysteresis ±0.26%).

[l]Measured using 13-point IV sweep with constant bias until data constant at 0.03% level.

[m]Initial efficiency. Krasovec[25] reviews the stability of similar devices.

[n]Spectral response and current-voltage curve reported in version 41 of these tables.

[o]Spectral response and current-voltage curve reported in version 46 of these tables.

[p]Spectral response and current-voltage curve reported in version 43 of these tables.

[q]Initial performance. Tanenbaum[26] and Krebs[27] review the stability of similar devices.

TABLE 2 "Notable exceptions" for single-junction cells and submodules: "top dozen" confirmed results, not class records, measured under the global AM1.5 spectrum (1000 Wm^{-2}) at 25°C (IEC 60904-3: 2008, ASTM G-173-03 global)

Classification	Efficiency (%)	Area (cm^2)	V_{oc} (V)	J_{sc} (mA/cm^2)	Fill Factor (%)	Test Centre (Date)	Description
Cells (silicon)							
Si (crystalline)	25.0 ± 0.5	4.00 (da)	0.706	42.7[a]	82.8	Sandia (March 9)[b]	UNSW p-type PERC top/rear contacts[28]
Si (crystalline)	25.8 ± 0.5[c]	4.008 (da)	0.7241	42.87[d]	83.1	FhG-ISE (August 17)	FhG-ISE, n-type top/rear contacts[29]
Si (crystalline)	**26.1 ± 0.3**[c]	**3.9857 (da)**	**0.7266**	**42.62**[e]	**84.3**	**ISFH (February 18)**	**ISFH, p-type rear IBC**[30]
Si (large)	26.6 ± 0.5	179.74 (da)	0.7403	42.5[f]	84.7	FhG-ISE (November 16)	Kaneka, n-type rear IBC[3]
Si (multicrystalline)	22.0 ± 0.4	245.83 (t)	0.6717	40.55[d]	80.9	FhG-ISE (November 17)	Jinko solar, large p-type[31]
GaInP	21.4 ± 0.3	0.2504 (ap)	1.4932	16.31[g]	87.7	NREL (November 16)	LG electronics, high bandgap[32]
GaInAsP/GaInAs	32.6 ± 1.4[c]	0.248 (ap)	2.024	19.51[d]	82.5	NREL (October 17)	NREL, monolithic tandem[33]
Cells (chalcogenide)							
CdTe (thin film)	22.1 ± 0.5	0.4798 (da)	0.8872	31.69[h]	78.5	Newport (November 15)	First solar on glass[34]
CZTSS (thin film)	12.6 ± 0.3	0.4209 (ap)	0.5134	35.21[i]	69.8	Newport (August 13)	IBM solution grown[35]
CZTS (thin film)	11.0 ± 0.2	0.2339 (da)	0.7306	21.74[f]	69.3	NREL (March 17)	UNSW on glass[13]
Cells (other)							
Perovskite (thin film)	22.7 ± 0.8[j,k]	0.0935 (ap)	1.144	24.92[d]	79.6	Newport (July 17)	KRICT[16]
Organic (thin film)	**12.3 ± 0.3**[l,m]	**0.0900 (da)**	**0.8870**	**18.83**[e]	**73.5**	**Newport (February 18)**	**BHJ OPV, PPC/CAS**[36]

CIGSS, CuInGaSSe; CZTSS, $Cu_2ZnSnS_{4-y}Se_y$; CZTS, Cu_2ZnSnS_4; ap, aperture area; t, total area; da, designated illumination area; AIST, Japanese National Institute of Advanced Industrial Science and Technology; NREL, National Renewable Energy Laboratory; FhG-ISE, Fraunhofer-Institut für Solare Energiesysteme; ISFH, Institute for Solar Energy Research, Hamelin.

[a]Spectral response reported in version 36 of these tables.

[b]Recalibrated from original measurement.

[c]Not measured at an external laboratory.

[d]Spectral response and current-voltage curves reported in version 51 of these tables.

[e]Spectral response and current-voltage curve reported in the present version of these tables.

[f]Spectral response and current-voltage curves reported in version 50 of these tables.

[g]Spectral response and current-voltage curves reported in version 49 of these tables.

[h]Spectral response and/or current-voltage curves reported in version 46 of these tables.

[i]Spectral response and current-voltage curves reported in version 44 of these tables.

[j]Stability not investigated. Han[23] and Yang and You[24] document stability of similar devices.

[k]Average of forward and reverse sweep at 150 mV/second (hysteresis ±0.51%).

[l]Long term stability not investigated. Tanenbaum[26] and Krebs[27] document stability of similar devices.

[m]Measured using a 13-point IV sweep with constant bias until data constant at 0.05% level.

TABLE 3 Confirmed multiple-junction terrestrial cell and submodule efficiencies measured under the global AM1.5 spectrum (1000 W/m^2) at 25°C (IEC 60904-3: 2008, ASTM G-173-03 global)

Classification	Efficiency (%)	Area (cm^2)	V_{oc} (V)	J_{sc} (mA/cm^2)	Fill Factor (%)	Test Centre (Date)	Description
III-V multijunctions							
5 Junction cell (bonded) (2.17/1.68/1.40/1.06/0.73 eV)	38.8 ± 1.2	1.021 (ap)	4.767	9.564	85.2	NREL (7/13)	Spectrolab, 2-terminal[37]
InGaP/GaAs/InGaAs	37.9 ± 1.2	1.047 (ap)	3.065	14.27[a]	86.7	AIST (2/13)	Sharp, 2 term[38]
GaInP/GaAs (monolithic)	32.8 ± 1.4	1.000 (ap)	2.568	14.56[b]	87.7	NREL (9/17)	LG electronics, 2 term.
Multijunctions with c-Si							
GaInP/GaAs/Si (mech. stack)	35.9 ± 0.5[c]	1.002 (da)	2.52/0.681	13.6/11.0	87.5/78.5	NREL (2/17)	NREL/CSEM/EPFL, 4-term.[39]
GaInP/GaAs/Si (wafer bonded)	33.3 ± 1.2[c]	3.984 (ap)	3.127[b]	12.7[b]	83.5	FhG-ISE (8/17)	Fraunhofer ISE, 2-term.[40]
GaAsP/Si (monolithic)	**20.1 ± 1.3**	**3.940 (ap)**	**1.673**	**14.94[e]**	**80.3**	**NREL (5/18)**	**OSU/SolAero/UNSW, 2-term.**
GaAs/Si (mech. stack)	32.8 ± 0.5[c]	1.003 (da)	1.09/0.683	28.9/11.1[e]	85.0/79.2	NREL (12/16)	NREL/CSEM/EPFL, 4-term.[39]
Perovskite/Si (monolithic)	**25.2 ± 0.7[f]**	**1.419 (da)**	**1.787**	**19.53[d]**	**72.3**	**FhG-ISE (2/18)**	**EPFL, 2-term.[41]**
Perovskite/Si (monolithic)	**25.2 ± 0.8[f]**	**1.088 (da)**	**1.793**	**19.02[d]**	**73.8**	**FhG-ISE (4/18)**	**Oxford PV/Oxford/HZB[42]**
GaInP/GaInAs/Ge; Si (spectral split minimodule)	34.5 ±2.0	27.83 (ap)	2.66/0.65	13.1/9.3	85.6/79.0	NREL (4/16)	UNSW/Azur/Trina, 4-term.[43]
a-Si/nc-Si multijunctions							
a-Si/nc-Si/nc-Si (thin film)	14.0 ± 0.4[g,c]	1.045 (da)	1.922	9.94[h]	73.4	AIST (5/16)	AIST, 2-term.[44]
a-Si/nc-Si (thin-film cell)	12.7 ± 0.4[g,c]	1.000 (da)	1.342	13.45[i]	70.2	AIST (10/14)	AIST, 2-term.[14,15]
Notable exception							
Perovskite/CIGS[j]	**22.4 ± 1.9[f]**	**0.042 (da)**	**1.774**	**17.3[d]**	**73.1**	**NREL (11/17)**	**UCLA, 2-term.[45]**

a-Si, amorphous silicon/hydrogen alloy; nc-Si, nanocrystalline or microcrystalline silicon; ap, aperture area; t, total area; da, designated illumination area; FhG-ISE, Fraunhofer Institut für Solare Energiesysteme; AIST, Japanese National Institute of Advanced Industrial Science and Technology.

[a]Spectral response and current-voltage curve reported in version 42 of these tables.

[b]Spectral response and current-voltage curve reported in the version 51 of these tables.

[c]Not measured at an external laboratory.

[d]Spectral response and current-voltage curve reported in the present version of these tables.

[e]Spectral response and current-voltage curve reported in version 50 of these tables.

[f]Initial efficiency. Han[23] and Yang and You[24] review the stability of similar perovskite-based devices.

[g]Stabilized by 1000-hour exposure to 1-sun light at 50 C.

[h]Spectral response and current-voltage curve reported in version 49 of these tables.

[i]Spectral responses and current-voltage curve reported in version 45 of these tables.

[j]Area too small to qualify as outright class record.

TABLE 4 Confirmed terrestrial module efficiencies measured under the global AM1.5 spectrum (1000 W/m^2) at a cell temperature of 25°C (IEC 60904-3: 2008, ASTM G-173-03 global)

Classification	Effic. (%)	Area (cm^2)	V_{oc} (V)	I_{sc} (A)	FF (%)	Test Centre (Date)	Description
Si (crystalline)	24.4 ± 0.5	13177 (da)	79.5	5.04[a]	80.1	AIST (September 16)	Kaneka (108 cells)[3]
Si (multicrystalline)	19.9 ± 0.4	15143 (ap)	78.87	4.795[a]	79.5	FhG-ISE (October 16)	Trina solar (120 cells)[46]
GaAs (thin film)	25.1 ± 0.8	866.45 (ap)	11.08	2.303[b]	85.3	NREL (November 17)	Alta devices[47]
CIGS (cd free)	19.2 ± 0.5	841 (ap)	48.0	0.456[b]	73.7	AIST (January 17)	Solar frontier (70 cells)[48]
CdTe (thin film)	18.6 ± 0.5	7038.8 (da)	110.6	1.533[d]	74.2	NREL (April 15)	First solar, monolithic[49]
a-Si/nc-Si (tandem)	12.3 ± 0.3[f]	14322 (t)	280.1	0.902[f]	69.9	ESTI (September 14)	TEL solar, Trubbach labs[50]
Perovskite	**11.6 ± 0.4**[g]	**802 (da)**	**23.79**	**0.577**[h]	**68.0**	**AIST (April 18)**	**Toshiba (22 cells)**[18]
Organic	8.7 ± 0.3[h]	802 (da)	17.47	0.569[d]	70.4	AIST (May 14)	Toshiba[22]
Multijunction							
InGaP/GaAs/InGaAs	31.2 ± 1.2	968 (da)	23.95	1.506	83.6	AIST (February 16)	Sharp (32 cells)[47,51]
Notable exception							
CIGS (large)	15.7 ± 0.5	9703 (ap)	28.24	7.254[i]	72.5	NREL (November 10)	Miasole[52]

CIGSS, CuInGaSSe; a-Si, amorphous silicon/hydrogen alloy; a-SiGe, amorphous silicon/germanium/hydrogen alloy; nc-Si, nanocrystalline or microcrystalline silicon; Effic., efficiency; t, total area; ap, aperture area; da, designated illumination area; FF, fill factor.

[a]Spectral response and current-voltage curve reported in version 49 of these tables.

[b]Spectral response and current-voltage curve reported in version 50 or 51 of these tables.

[c]Spectral response and/or current-voltage curve reported in version 47 of these tables.

[d]Spectral response and current-voltage curve reported in version 45 of these tables.

[e]Stabilized at the manufacturer to the 2% level following IEC procedure of repeated measurements.

[f]Spectral response and/or current-voltage curve reported in version 46 of these tables.

[g]Initial performance. Han[23] and Yang and You[24] review the stability of similar devices.

[h]Spectral response and current-voltage curve reported in the present version of these tables.

[i]Spectral response reported in version 37 of these tables.

TABLE 5 Terrestrial concentrator cell and module efficiencies measured under the ASTM G-173-03 direct beam AM1.5 spectrum at a cell temperature of 25°C

Classification	Effic. (%)	Area (cm^2)	Intensity (suns)	Test Centre (Date)	Description
Single cells					
GaAs	29.3 ± 0.7[b]	0.09359 (da)	49.9	NREL (October 16)	LG electronics
Si	27.6 ± 1.2[c]	1.00 (da)	92	FhG-ISE (November 04)	Amonix back-contact[53]
CIGS (thin film)	23.3 ± 1.2[d,e]	0.09902 (ap)	15	NREL (March 14)	NREL[54]
Multijunction cells					
GaInP/GaAs; GaInAsP/GaInAs	46.0 ± 2.2[f]	0.0520 (da)	508	AIST (October 14)	Soitec/CEA/FhG-ISE 4j bonded[55]
GaInP/GaAs/GaInAs/GaInAs	45.7± 2.3[d,g]	0.09709 (da)	234	NREL (September 14)	NREL, 4j monolithic[56]
InGaP/GaAs/InGaAs	44.4 ± 2.6[h]	0.1652 (da)	302	FhG-ISE (April 13)	Sharp, 3j inverted metamorphic[57]
GaInAsP/GaInAs	35.5 ± 1.2[i,d]	0.10031 (da)	38	NREL (October 17)	NREL 2-junction (2j)[29]
Minimodule					
GaInP/GaAs; GaInAsP/GaInAs	43.4 ± 2.4[d,j]	18.2 (ap)	340[k]	FhG-ISE (July 15)	Fraunhofer ISE 4j (lens/cell)[58]
Submodule					
GaInP/GaInAs/Ge; Si	40.6 ± 2.0[j]	287 (ap)	365	NREL (April 16)	UNSW 4j split spectrum[59]
Modules					
S i	20.5 ± 0.8[d]	1875 (ap)	79	Sandia (April 89)[l]	Sandia/UNSW/ENTECH (12 cells)[60]
Three junction (3j)	35.9 ± 1.8[m]	1092 (ap)	N/A	NREL (August 13)	Amonix[61]
Four junction (4j)	38.9 ± 2.5[n]	812.3 (ap)	333	FhG-ISE (April 15)	Soitec[62]
"Notable exceptions"					
Si (large area)	21.7 ± 0.7	20.0 (da)	11	Sandia (September 90)[k]	UNSW laser grooved[63]
Luminescent minimodule	7.1 ± 0.2	25 (ap)	2.5[k]	ESTI (September 08)	ECN Petten, GaAs cells[64]

CIGS, $CuInGaSe_2$; Effic., efficiency; da, designated illumination area; ap, aperture area; NREL, National Renewable Energy Laboratory; FhG-ISE, Fraunhofer-Institut für Solare Energiesysteme.

[a]One sun corresponds to direct irradiance of 1000 Wm^{-2}.

[b]Spectral response and current-voltage curve reported in version 50 of these tables.

[c]Measured under a low aerosol optical depth spectrum similar to ASTM G-173-03 direct.[65]

[d]Not measured at an external laboratory.

[e]Spectral response and current-voltage curve reported in version 44 of these tables.

[f]Spectral response and current-voltage curve reported in version 45 of these tables.

[g]Spectral response and current-voltage curve reported in version 46 of these tables.

[h]Spectral response and current-voltage curve reported in version 42 of these tables.

[i]Spectral response and current-voltage curve reported in version 51 of these tables.

[j]Determined at IEC 62670-1 CSTC reference conditions.

[k]Geometric concentration.

[l]Recalibrated from original measurement.

[m]Referenced to 1000 W/m^2 direct irradiance and 25°C cell temperature using the prevailing solar spectrum and an in-house procedure for temperature translation.

[n]Measured under IEC 62670-1 reference conditions following the current IEC power rating draft 62670-3.

nominally 12 entries with the present authors having voted for their preferences for inclusion. Readers who have suggestions of notable exceptions for inclusion into this or subsequent tables are welcome to contact any of the authors with full details. Suggestions conforming to the guidelines will be included on the voting list for a future issue.

Table 3 is first introduced in version 49 of these tables and summarizes the growing number of cell and submodule results involving high efficiency, 1-sun multiple-junction devices (previously reported in Table 1). Table 4 shows the best results for 1-sun modules, both single and multiple junction, while Table 5 shows the best results for concentrator cells and concentrator modules. A small number of notable exceptions are also included in Tables 3–5.

2 | NEW RESULTS

Ten new results are reported in the present version of these tables. The first new result in Table 1 is a new record for any thin-film polycrystalline solar cell with an efficiency of 22.9% measured for a 1-cm^2 CIGS ($CuIn_{1-x}Ga_xSe_2$) solar cell fabricated by Solar Frontier[10,11] and measured by the Japanese National Institute of Advanced Industrial Science and Technology (AIST).

The second new result is a new efficiency record for a perovskite minimodule. An efficiency of 17.25% is reported for a 19-cm^2 minimodule fabricated by Microquanta Semiconductor[17] and measured at the Newport PV Laboratory. For perovskite cells, the tables now accept results based on "quasi-steady-state" measurements (sometimes called "stabilized" in the perovskite field, although this conflicts with usage in other areas of photovoltaics). Along with other emerging technologies, perovskite cells may not demonstrate the same level of stability as conventional cells, with the stability of perovskite cells discussed elsewhere.[62,63]

A third new result in Table 1 is 11.7% efficiency for a relatively large-area 703-cm^2 perovskite submodule fabricated by Toshiba[18] and measured at AIST (200 cm^2 is the minimal area requirement for this category). The device was prepared on a resin film fixed on a glass plate and then sealed with a second glass plate.

The first of 2 new results in Table 2 (notable exceptions) represents an outright 1-sun record for a silicon cell using a p-type substrate, with an efficiency of 26.1% confirmed for a 4-cm^2 cell fabricated by the Institute for Solar Energy Research, Hamelin and measured at the Institute's Calibration and Test Center. The cell uses an interdigitated back contact (IBC) structure fabricated on a p-type, float zone Si wafer with passivating poly-Si on oxide contacts for both polarities on the cell rear.[30]

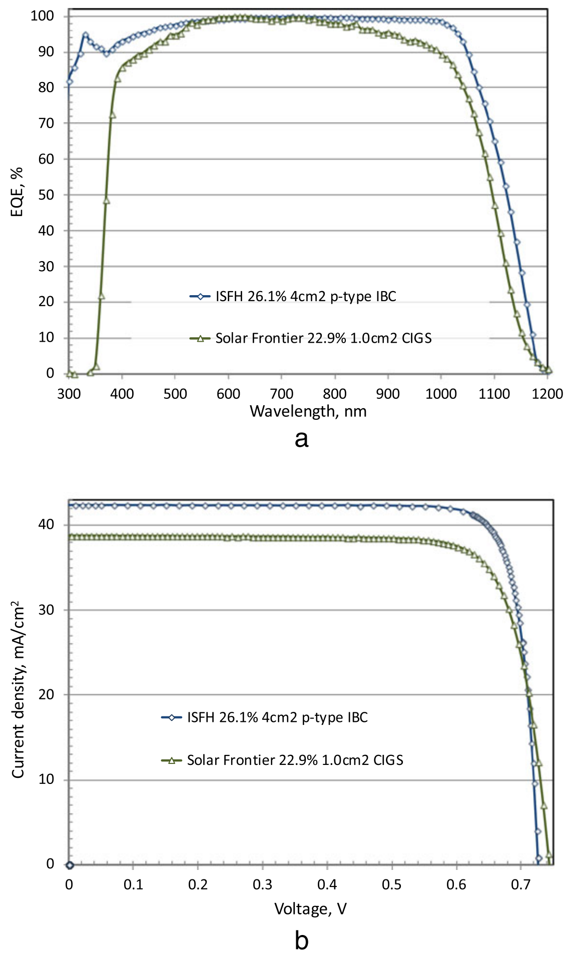

FIGURE 1 A, External quantum efficiency for the new silicon and $CuIn_{1-x}Ga_xSe_2$ cell results reported in this issue (results normalized). B, Corresponding current density-voltage (JV) curves for the same devices [Colour figure can be viewed at wileyonlinelibrary.com]

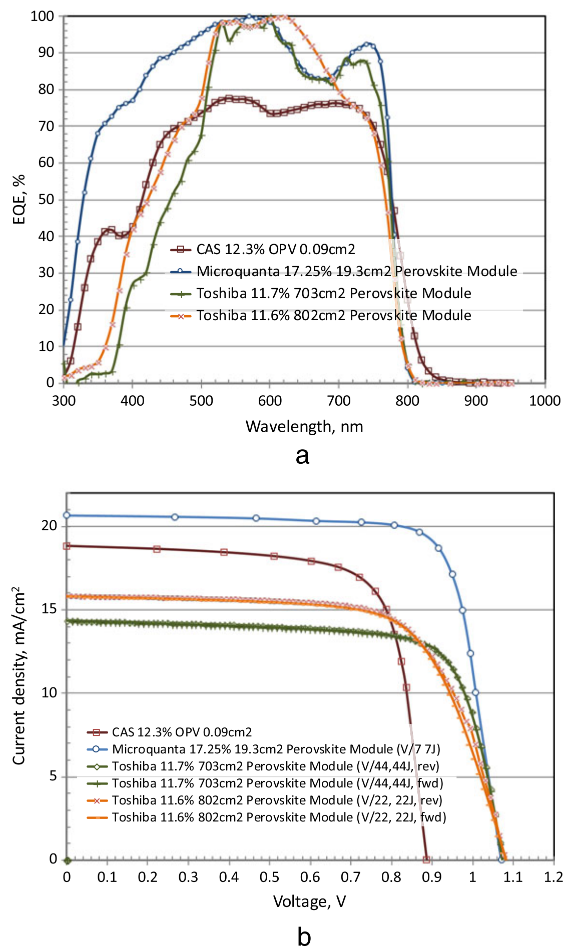

FIGURE 2 A, External quantum efficiency for the new OPV cell results and perovskite module results reported in this issue (some results normalized). B, Corresponding current density-voltage (JV) curves [Colour figure can be viewed at wileyonlinelibrary.com]

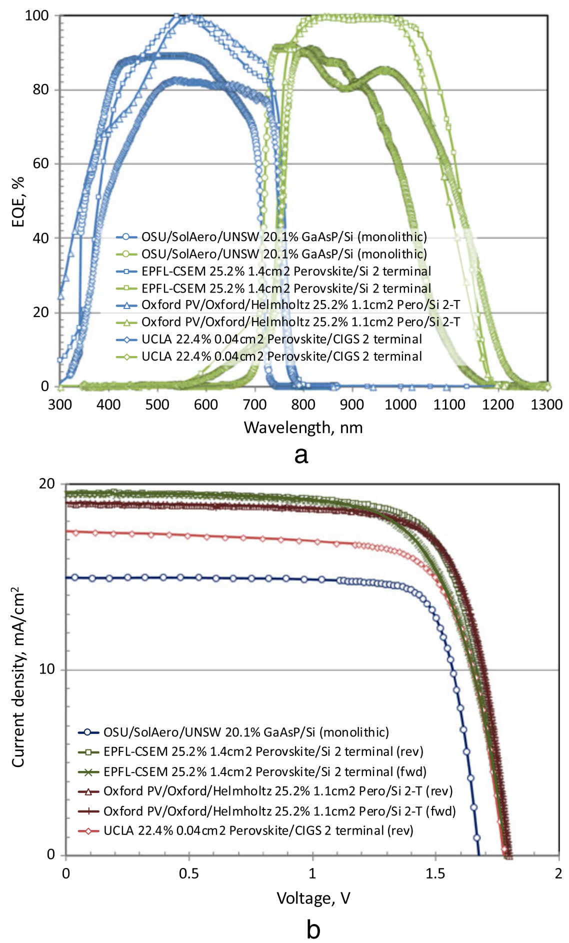

FIGURE 3 A External quantum efficiency for the new 2-junction, 2-terminal cell results reported in this issue (some results normalized). B, Corresponding current density-voltage (JV) curves [Colour figure can be viewed at wileyonlinelibrary.com]

A second new notable exception in Table 2 is 12.3% for a small area 0.09-cm^2 bulk heterojunction organic solar cell (BHJ OPV) based on polymer donor and small molecule acceptor material. The cell was fabricated at the State Key Laboratory of Polymer Physics and Chemistry of the Chinese Academy of Science (PPC/CAS)[18] and measured at Newport. The stability of organic solar cells is discussed elsewhere.[26,27] Cell area is also too small for classification as an outright record, with solar cell efficiency targets in governmental research programs generally specified in a cell area of 1 cm^2 or larger.[66-68]

Four new results are reported in Table 3 relating to 1-sun, multijunction devices. The first is for a 4-cm^2 monolithic, 2-junction, 2-terminal GaAsP/Si tandem device fabricated by a joint effort of Ohio State University (OSU), SolAero Technologies Corporation and the University of New South Wales, Sydney (UNSW) and measured at the US National Renewable Energy Laboratory (NREL).

Two more new results report the demonstration of the same efficiency of 25.2% for perovskite/silicon monolithic 2-junction, 2-terminal devices, with both results measured at the Fraunhofer Institute for Solar Energy Systems. The first is for a 1.4-cm^2 device fabricated by the PV Labs of the École Polytechnique Fédérale de Lausanne (EPFL),[41] while the second is for a 1.1-cm^2 device fabricated by a collaborative effort of Oxford PV, the University of Oxford, and Helmholtz Zentrum Berlin (HZB).[42]

A fourth new result for Table 3 is included as a multijunction cell notable exception, because the area is too small for classification as an outright class record. An efficiency of 22.4% was measured for a small area 0.04-cm^2 perovskite/CIGS monolithic 2-junction, 2-terminal cell fabricated by University of California, Los Angeles (UCLA)[45] and measured at NREL.

Despite implications to the contrary, none of our test centers are presently able to confirm the claimed 14.7% tandem OPV cell efficiency recently reported in a high-profile journal.[69]

One new module result is reported in Table 4. An efficiency of 11.6% has been confirmed for a 802-cm^2 perovskite module fabricated by Toshiba[18] and measured by AIST.

The EQE spectra for the new silicon and CIGS cell results reported in the present issue of these tables are shown in Figure 1A, with Figure 1B showing the current density-voltage (JV) curves for the same devices. Figure 2A shows the EQE for the new OPV cell and perovskite module results with Figure 2B showing their current density-voltage (JV) curves. Figures 3A and 3B show the corresponding EQE and JV curves for the new 2-junction, 2-terminal cell results.

DISCLAIMER

While the information provided in the tables is provided in good faith, the authors, editors, and publishers cannot accept direct responsibility for any errors or omissions.

ACKNOWLEDGEMENTS

The Australian Centre for Advanced Photovoltaics commenced operation in February 2013 with support from the Australian Government through the Australian Renewable Energy Agency (ARENA). The Australian Government does not accept responsibility for the views, information, or advice expressed herein. The work by D. Levi was supported by the US Department of Energy under contract no. DE-AC36-08-GO28308 with the National Renewable Energy Laboratory. The work at AIST was supported in part by the Japanese New Energy and Industrial Technology Development Organization (NEDO) under the Ministry of Economy, Trade and Industry (METI).

ORCID

Martin A. Green http://orcid.org/0000-0002-8860-396X
Yoshihiro Hishikawa http://orcid.org/0000-0002-8420-9260
Anita W.Y. Ho-Baillie http://orcid.org/0000-0001-9849-4755

REFERENCES

1. Green MA, Emery K, Hishikawa Y, et al. Solar cell efficiency tables (version 51). *Prog Photovolt Res Appl*. 2018;26(1):3-12.
2. Green MA, Emery K, Hishikawa Y, Warta W. Solar cell efficiency tables (version 33). *Prog Photovolt Res Appl*. 2009;17(1):85-94.
3. Yoshikawa K, Kawasaki H, Yoshida W, et al. Silicon heterojunction solar cell with interdigitated back contacts for a photoconversion efficiency over 26%. *Nature Energy*. 2017;2(5):17032.
4. Benick J, Richter A, Müller R, et al. High-efficiency n-type HP mc silicon solar cells. *IEEE J Photovoltaics*. 2017;7(5):1171-1175.
5. Moslehi MM, Kapur P, Kramer J, Rana V, Seutter S, Deshpande A, Stalcup T, Kommera S, Ashjaee J, Calcaterra A, Grupp D, Dutton D, Brown R. World-record 20.6% efficiency 156 mm x 156 mm full-

square solar cells using low-cost kerfless ultrathin epitaxial silicon & porous silicon lift-off technology for industry-leading high-performance smart PV modules. *PV Asia Pacific Conference (APVIA/PVAP)*, 24 October 2012.

6. Keevers MJ, Young TL, Schubert U, Green MA. 10% efficient CSG minimodules. *22nd European Photovoltaic* Solar Energy *Conference*, Milan, September 2007.
7. Kayes BM, Nie H, Twist R, Spruytte SG, Reinhardt F, Kizilyalli IC, Higashi GS. 27.6% conversion efficiency, a new record for single-junction solar cells under 1 sun illumination. *Proceedings of the 37th IEEE Photovoltaic Specialists Conference*, 2011.
8. Venkatasubramanian R, O'Quinn BC, Hills JS, Sharps PR, Timmons ML, Hutchby JA, Field H, Ahrenkiel A, Keyes B. 18.2% (AM1.5) efficient GaAs solar cell on optical-grade polycrystalline Ge substrate. *Conference Record, 25th IEEE Photovoltaic Specialists Conference*, Washington, May 1997, 31–36.
9. Wanlass M. Systems and methods for advanced ultra-high-performance InP solar Cell US Patent 9,590,131 B2, 7 March 2017.
10. Solar Frontier Press Release dated 20 December 2017, "Solar Frontier Achieves World Record Thin-Film Solar Cell Efficiency of 22.9%" (http://www.solar-frontier.com/eng/news/2017/1220_press.html, accessed 9 May 2018).
11. Wu JL, Hirai Y, Kato T, Sugimoto H, Bermudez V. New world Record efficiency up to 22.9% for Cu (In,Ga)(Se,S)$_2$ thin-film solar cell *7th World Conference on Photovoltaic* Energy Conversion *(WCPEC-7)*, June 10–15, 2018, Waikoloa, HI, USA.
12. First Solar Press Release, First Solar builds the highest efficiency thin film PV cell on record, 5 August 2014.
13. Sun K, Yan C, Liu F, et al. Beyond 9% efficient kesterite Cu2ZnSnS4 solar cell: Fabricated by using Zn1-xCdxS buffer layer. *Adv Energy Mater*. 2016;6(12):1600046. https://doi.org/10.1002/aenm.201600046
14. Matsui T, Bidiville A, Sai H, et al. High-efficiency amorphous silicon solar cells: Impact of deposition rate on metastability. *Appl Phys Lett*. 2015;106:053901. https://doi.org/10.1063/1.4907001
15. Sai H, Maejima K, Matsui T, et al. High-efficiency microcrystalline silicon solar cells on honeycomb textured substrates grown with high-rate VHF plasma-enhanced chemical vapor deposition. *Jpn J Appl Phys*. 2015;54(8S1):08KB05.
16. Yang WS, Noh JH, Jeon NJ, et al. High-performance photovoltaic perovskite layers fabricated through intramolecular exchange. *Science*. 2015;348(6240):1234-1237.
17. http://www.microquanta.com (accessed 9 May, 2018).
18. Toshiba news release dated 25 September 2017 (https://www.toshiba.co.jp/rdc/rd/detail_e/e1709_02.html)
19. Komiya R, Fukui A, Murofushi N, Koide N, Yamanaka R and Katayama H. Improvement of the conversion efficiency of a monolithic type dye-sensitized solar cell module. *Technical Digest, 21st International Photovoltaic* Science *and* Engineering Conference, Fukuoka, November 2011; 2C-5O-08.
20. Kawai M. High-durability dye improves efficiency of dye-sensitized solar cells. Nikkei Electronics 2013; Feb.1 (http://techon.nikkeibp.co.jp/english/NEWS_EN/20130131/263532/) (accessed 23 October, 2013)
21. Mori S, Oh-oka H, Nakao H, et al. Organic photovoltaic module development with inverted device structure. *MRS Proc*. 2015;1737. https://doi.org/10.1557/opl.2015.540
22. Hosoya M, Oooka H, Nakao H, Gotanda T, Mori S, Shida N, Hayase R, Nakano Y, Saito M. Organic thin film photovoltaic modules. Proceedings of the 93rd Annual Meeting of the Chemical Society of Japan 2013; 21–37.
23. Han Y, Meyer S, Dkhissi Y, et al. Degradation observations of encapsulated planar $CH_3NH_3PbI_3$ perovskite solar cells at high temperatures and humidity. *J Mater Chem A*. 2015;3(15):8139-8147.
24. Yang Y, You J. Make perovskite solar cells stable. *Nature*. 2017;544(7649):155-156.
25. Krašovec UO, Bokalič M, Topič M. Ageing of DSSC studied by electroluminescence and transmission imaging. *Sol Energy Mater Sol Cells*. 2013;117:67-72.
26. Tanenbaum DM, Hermenau M, Voroshazi E, et al. The ISOS-3 interlaboratory collaboration focused on the stability of a variety of organic photovoltaic devices. *RSC Adv*. 2012;2(3):882-893.
27. Krebs FC (Ed). Stability and degradation of organic and polymer solar cells, *Wiley, Chichester*, 2012; Jorgensen M, Norrman K, Gevorgyan SA, Tromholt T, Andreasen B, Krebs FC. Stability of polymer solar cells. *Adv Mater*. 2012;24:580-612.
28. Zhao J, Wang A, Green MA, Novel FF. 19.8% efficient "honeycomb" textured multicrystalline and 24.4% monocrystalline silicon solar cells. *Appl Phys Lett*. 1998;73(14):1991-1993.
29. Richter A, Benick J, Feldmann F, Fell A, Hermle M, Glunz SW. N-type Si solar cells with passivating electron contact: Identifying sources for efficiency limitations by wafer thickness and resistivity variation. *Sol Energy Mater Sol Cells*. 2017;173:96-105.
30. Haase F, Klamt C, Schäfer S, et al. Laser contact openings in dielectric layers for local poly-Si-metal contacts. *Sol Energy Mater Sol Cells*. 2018. (accepted for publication)
31. https://www.jinkosolar.com/press_detail_1380.htm (accessed 9 May, 2018).
32. Kim S, Hwang ST, Yoon W, Lee HM. High performance GaAs solar cell using heterojunction emitter and its further improvement by ELO technique. Paper 4CV.1.27, *European Photovoltaic Solar Energy Conference* 2016, Munich, June 2016.
33. Jain N, Schulte KL, Geisz JF, et al. High-efficiency inverted metamorphic 1.7/1.1eV GainAsP/GaInAs dual junction solar cells. *Appl Phys Lett*. 2018;112(5):053905.
34. First Solar Press Release. First Solar Achieves yet another cell conversion efficiency world record, 24 February 2016.
35. Wang W, Winkler MT, Gunawan O, et al. Device characteristics of CZTSSe thin-film solar cells with 12.6% efficiency. *Adv Energy Mater*. 2013. https://doi.org/10.1002/aenm. 201301465
36. http://polymer.iccas.ac.cn/en/introduction.asp
37. Chiu PT, Law DL, Woo RL, Singer S, Bhusari D, Hong WD, Zakaria A, Boisvert JC, Mesropian S, King RR, Karam NH. 35.8% space and 38.8% terrestrial 5J direct bonded cells. *Proc. 40th IEEE Photovoltaic Specialist Conference*, Denver, June 2014; 11–13.
38. Sasaki K, Agui T, Nakaido K, Takahashi N, Onitsuka R, Takamoto T. Proceedings, 9th International Conference on Concentrating Photovoltaics Systems, Miyazaki, Japan 2013.
39. Essig S, Allebé C, Remo T, et al. Raising the one-sun conversion efficiency of III–V/Si solar cells to 32.8% for two junctions and 35.9% for three junctions. *Nature Energy*. 2017;2(9):17144. https://doi.org/10.1038/nenergy.2017.144
40. https://www.ise.fraunhofer.de/content/dam/ise/en/documents/News/2017/0917_News_31_Percent_for-Silicon-based-multi-junction-solar-cell_e.pdf
41. https://pvlab.epfl.ch
42. https://www.oxfordpv.com/news/oxford-pv-collaborates-hzb-move-peroskite-solar-cells-closer-commercialisation
43. Green MA, Keevers MJ, Concha Ramon B, Jiang Y, Thomas I, Lasich JB, Verlinden, PJ, Yang Y, Zhang X, Emery K, Moriarty T, King RR, Bensch W. Improvements in sunlight to electricity conversion efficiency: above 40% for Director sunlight and over 30% for global. Paper 1AP.1.2, *European Photovoltaic* Solar Energy *Conference* 2015, Hamburg, September 2015.
44. Sai H, Matsui T, Koida T, et al. Triple-junction thin-film silicon solar cell fabricated on periodically textured substrate with a stabilized efficiency of 13.6%. *Appl Phys Lett*. 2015;106(21):213902. https://doi.org/10.1063/1.4921794
45. http://yylab.seas.ucla.edu

46. Verlinden PJ, et al. Will we have >22% efficient multi-crystalline Silicon solar Cell? *PVSEC 26*, Singapore, 24–28 October, 2016.
47. Mattos LS, Scully SR, Syfu M, Olson E, Yang L, Ling C, Kayes BM, He G. New module efficiency record: 23.5% under 1-sun illumination using thin-film single-junction GaAs solar cells. *Proceedings of the 38th IEEE Photovoltaic Specialists Conference*, 2012.
48. Sugimoto H. High efficiency and large volume production of CIS-based modules. *40th IEEE Photovoltaic Specialists Conference*, Denver, June 2014.
49. First Solar Press Release. First Solar achieves world Record 18.6% thin film module conversion efficiency, 15 June 2015.
50. Cashmore JS, Apolloni M, Braga A, et al. Improved conversion efficiencies of thin-film silicon tandem (MICROMORPH ™) photovoltaic modules. *Sol Energy Mater Sol Cells*. 2016;144:84-95. https://doi.org/10.1016/j.solmat. 2015.08.022
51. Takamoto T. Application of InGaP/GaAs/InGaAs triple junction solar cells to space use and concentrator photovoltaic. *40th IEEE Photovoltaic Specialists Conference*, Denver, June 2014.
52. http://www.miasole.com (accessed 22 May, 2015).
53. Slade A, Garboushian V. 27.6% efficient silicon concentrator cell for mass production. *Technical Digest*, *15th International Photovoltaic* Science *and* Engineering Conference, Shanghai, October 2005; 701.
54. Ward JS, Ramanathan K, Hasoon FS, et al. A 21.5% efficient cu (in,Ga) Se2 thin-film concentrator solar cell. *Prog Photovolt Res Appl*. 2002;10(1):41-46.
55. Press Release, Fraunhofer Institute for Solar Energy Systems, 1 December 2014 (accessed at http://www.ise.fraunhofer.de/en/press-and-media/press-releases/press-releases-2014/new-world-record-for-solar-cell-efficiency-at-46-percent on 7 December 2014).
56. NREL Press Release NR-4514, 16 December 2014.
57. Press Release, Sharp Corporation, 31 May 2012 (accessed at http://sharp-world.com/corporate/news/120531.html on 5 June 2013).
58. Steiner M, Siefer G, Schmidt T, Wiesenfarth M, Dimroth F, Bett AW. 43 % Sun light to electricity conversion efficiency using CPV. *IEEE Journal of Photovoltaics*, submitted.
59. Green MA, Keevers MJ, Thomas I, Lasich JB, Emery K, King RR. 40% efficient sunlight to electricity conversion. *Prog Photovolt Res Appl*. 2015;23(6):685-691.
60. Chiang CJ, Richards EH. A 20% efficient photovoltaic concentrator module. *Conf*. Record, *21st* IEEE *Photovoltaic Specialists Conference*, Kissimimee, May 1990: 861–863.
61. http://amonix.com/pressreleases/amonix-achieves-world-record-359-module-efficiency-rating-nrel-4 (accessed 23 October 2013).
62. van Riesen S, Neubauer M, Boos A, Rico MM, Gourdel C, Wanka S, Krause R, Guernard P, Gombert A. New module design with 4-junction solar cells for high efficiencies. Proceedings of the 11th Conference on Concentrator Photovoltaic Systems, 2015.
63. Zhang F, Wenham SR, Green MA. Large area, concentrator buried contact solar cells. *IEEE Trans Electron Devices*. 1995;42(1):144-149.
64. Slooff LH, Bende EE, Burgers AR, et al. A luminescent solar concentrator with 7.1% power conversion efficiency. *Phys Status Solidi (RRL)*. 2008;2(6):257-259.
65. Gueymard CA, Myers D, Emery K. Proposed reference irradiance spectra for solar energy systems testing. *Sol Energy*. 2002;73(6):443-467.
66. Program milestones and decision points for single junction thin films. *Annual Progress Report* 1984, *Photovoltaics*, *Solar Energy Research Institute*, *Report* DOE/CE-0128, June 1985; **7**.
67. Sakata I, Tanaka Y, Koizawa K. Japan's new National R&D Program for photovoltaics. Photovoltaic Energy Conversion, Conference Record of the 2006 *IEEE 4th World Conference*, Vol. 1, May 2008; 1–4.
68. Jäger-Waldau, A (Ed.). PVNET: European Roadmap for PV R&D, EUR 21087 EN, 2004.
69. Che XZ, Li YX, Qu Y, Forrest SR. High fabrication yield organic tandem photovoltaics combining vacuum- and solution processed subcells with 15% efficiency. *Nature Energy*. 2018;3(5):422-427. https://doi.org/10.1038/s41560-018-0134-z

How to cite this article: Green MA, Hishikawa Y, Dunlop ED, Levi DH, Hohl-Ebinger J, Ho-Baillie AWY. Solar cell efficiency tables (version 52). *Prog Photovolt Res Appl*. 2018;26:427–436. https://doi.org/10.1002/pip.3040